RSC Advances

ROYAL SOCIETY OF CHEMISTRY

www.rsc.org/advances

Cite this: DOI: 10.1039/c0xx00000x

www.rsc.org/xxxxxx

ARTICLE TYPE

Polarization Enhanced Multi-grains Boundaries Dendritic Micro-nano Structure α-Fe for Electromagnetic Absorption Application: Synthesis and Characterization

Zhenxing Yu, Zhongping Yao, Na Zhang, Zhaohua Jiang*

Received (in XXX, XXX) Xth XXXXXXXXX 20XX, Accepted Xth XXXXXXXXX 20XX
DOI: 10.1039/b000000x

In this paper, the multi-grains boundaries hierarchical dendritic micro-nano structure α-Fe were successfully synthesized in the electrolyte containing rare earth (RE) ions by the electric field-induced and electrochemical reduction method. The results show that the size of dendritic morphological samples decreases from about 10μm to about 6μm with the increase of RE ions concentration, and plentiful nano-sized particles generates on their surface due to the adsorption suppression effect of RE ions, which facilitates the great increase of BET surface area and the formation of abundant grain boundaries. All these RE-added dendritic α-Fe exhibit excellently enhanced electromagnetic absorption performance. The minimum reflection loss (RL) value (around -60 dB) of RE-added samples is twice as much as that of the unadded samples, and the absorption peak moves to the higher frequency range as the RE ions concentration is increasing. The widest absorption band (in which RL< -20 dB) of La-added samples grows to 2 GHz. We mainly ascribe the great enhancement of EMA performances to the unique structure characters such as the great surface area and abundant grain boundaries, which could affect the dielectric loss and magnetic loss of the absorbers. Not only has this work directly confirm the influence of the interface and grain boundaries on electromagnetic absorption performance, but also provided a new way to control the morphology and microstructure by RE ions.

Introduction

Due to the great impact of electromagnetic interference on both humans and the environment[1, 2], the electromagnetic shielding has been one of the most concerned matters in daily life. In general, the electromagnetic shielding is mainly realized by means of the reflection and absorption functions from the surface materials or coating. But only the electromagnetic absorption is the truly effective method to consume the electromagnetic energy. The mechanisms of electromagnetic absorption are different and complicated for different materials. The causes for electromagnetic absorption include dielectric loss and magnetic loss.[3, 4] Nowadays, more and more attentions from scientists are paid to the dielectric loss, especially to polarizations which play the pivotal role on dielectric loss of electromagnetic absorption[5]. In order to enlarge the dielectric loss, many scientists are forcing their attentions on two or more constituents composed composites of which not only could the complementarities between the dielectric loss and the magnetic loss be tuned, but also the polarization is enhanced dramatically. The insulator or dielectric/magnetic composites materials (such as Fe@SiO_2[6], Ni/SiO_2[7], Fe@ZnO[8], Fe_3O_4/TiO_2[9], Fe_3O_4/SnO_2[10] and so on[11-13]) could enhance the interfacial polarization, and effect the eddy current loss and the associated relaxation[8, 12]. Carbon/magnetic materials (such as graphene/Fe[14], porous carbon/Co[15], carbon nanotubes/$CoFe_2O_4$[16] and so on[17]) also could enhance interfacial polarization[18, 19] and improve electrical conductivity[20]. Polymers/magnetic or dielectric materials, especially the polyvinylidene fluoride composites materials[21, 22], are the novel materials recently appeared which could improve the relaxations and interfacial polarizations[23] more clearly by the formation of large dipoles, and further result in the Debye dipolar relaxation and Maxwell–Wagner relaxation and synergic effect[24, 25]. All of these composites consisted by different forms, such as coated, doped and hybrid, provide multiple interfaces and heteronanostructures which further change their dielectric properties, and contribute a great enhancement on electromagnetic absorption properties. Therefore, the great significance of polarization is obvious.

Micro-nanostructure iron metal materials are the most potential electromagnetic absorber due to their low price and excellent performance in high frequency range.[26-28] In previous work, we have synthesized the hierarchical dendritic micro-nano structure α-Fe electromagnetic absorber which exhibit excellent electromagnetic absorption performance.[29] Based on the huge positive effect of grains boundaries for the electromagnetic absorption performance discussed above, the motivation of this work is to further enhance the polarization for electromagnetic wave by increasing the interface and grain boundaries of dendritic micro-nano structure α-Fe. According to the reports in

the literature, the strong adsorption effect stemming from their special 4f atomic orbits of Rare earth (RE) ions in electrolyte could increase the nucleation rate, and refine grains.[30, 31] Therefore, in this work, RE ions (La^{3+} and Ce^{3+}) were added as additional agents into the electrolyte during the electrodeposition process, by which the smaller sized multi-grains boundaries hierarchical dendritic micro-nano structure α-Fe absorber were successfully synthesized. The morphology, structure and properties of the samples were also systematically studied. And meantime the relation between multi-grains boundaries structure and electromagnetic absorption performance was analyzed as well. This work not only provides an excellent idea to control the crystal growth under the electric field force in the electrolyte, but also extends the application of the RE elements dramatically.

Experimental Section

Multi-grains boundaries dendritic micro-nano structure α-Fe absorbers were fabricated through an electric field-induced and electrochemical reduction method under constant current mode which is reported in our previous work.[29, 32] The ambient anodic area contained 250 mL 0.1 mol Ł$^{-1}$ sulfuric acid solution. Meanwhile, the center cathode area contained 40 mL 1.0 mol Ł$^{-1}$ Iron (II) sulfate heptahydrate and a certain amount (0.25, 0.50, 1.00, 2.00 g Ł$^{-1}$) of lanthanum nitrate hexahydrate or cerium (IV) sulfate tetrahydrate mixed solution. (Actually, the cerium ions in the electrolyte are Ce^{3+}, because the Ce^{4+} ions were reduced to Ce^{3+} by Fe^{2+} in the electrolyte, $Ce^{4+}+Fe^{2+}=Ce^{3+}+Fe^{3+}$) Herein, we use the Fe-1La, Fe-2La, Fe-3La and Fe-4La (or Fe-1Ce, Fe-2Ce, Fe-3Ce and Fe-4Ce) as the symbols to stand for the RE-added dendritic α-Fe synthesized under different RE ions concentration, respectively. The current density and reaction time were 30 A cm^{-1} and 20 seconds, respectively. The black flocculent samples generated on copper electrode with the reaction going on were transferred into the centrifugal tube filled with oxygen-free deionized water and separated by ultrasonic. The products were washed and centrifuged three times with oxygen-free deionized water and ethanol respectively. Then, the final product was dried at 60 ℃ in vacuum.

The crystalline structure and composition of the samples were characterized by X-Ray Diffraction (D/max-rB, RICOH, Japan) and Inductively Coupled Plasma Optical Emission Spectrometry (ICP-OES, Optima 8300, PerkinElmper, America). Their morphology and microstructure were obtained by Scanning Electron Microscopy (FEI Quanta 200F, America), Transmission Electron Microscopy and High-Resolution Transmission Electron Microscopy (FEI Tecnai G2 F30, America). Nitrogen adsorption isotherm measurements were carried out at 77.3 K with a high-performance Surface Area Analyzer and Pore Size Analyzer (Quadrasorb SI, Quantachrome, America). The magnetic properties of dendritic α-Fe were examined on a Vibrating Sample Magnetometer (Lake Shore 7404, America). The complex permittivity and permeability of dendritic α-Fe were tested on a vector network analyzer (Agilent N5230A, America). The samples for electromagnetic absorption property testing were dispersed in paraffin homogeneously with a sample-to-paraffin mass ratio of 7: 3, and then the mixture was molded to an annular-shaped sample with 7.00 mm in external diameter, 3.01 mm in internal diameter and 3.0 mm in thickness.

Results and discussion

Figure 1 shows scanning electron microscopy (SEM) images of La-added and Ce-added dendritic micro-nano structured α-Fe samples. The Fe-1RE sample (as shown in Figure 1a and 1c) almost possesses the same size and morphology as the pure dendritic α-Fe (Figure S1)[29]. Moreover, SEM images of Fe-4RE and other RE-added samples (Figure S2) show that the leaf-like dendritic micro-nano structural morphologies become a little untidily and unordered, but they still keep the leaf-like shape. However, with the increase of RE concentration in the electrolyte, their lengths change significantly, decreasing from about 10 μm for Fe-1La to about 6 μm for Fe-4La (Figure 1a and 1b). Ce-added dendritic micro-nano structured α-Fe samples in Figure 1c and 1d present the similar tendency as La-added samples.

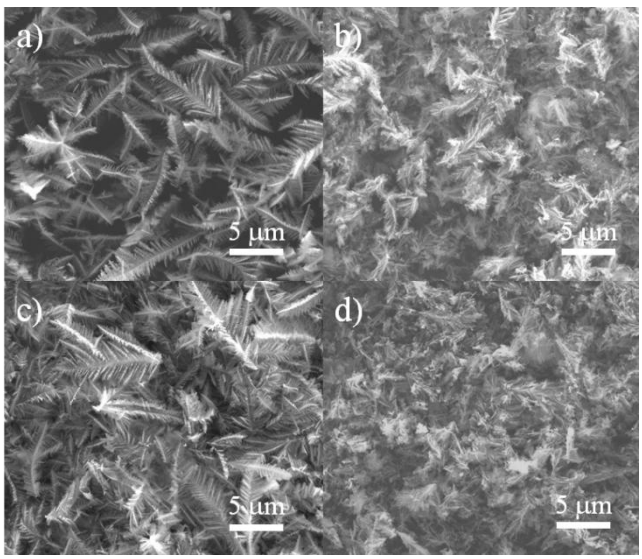

Fig.1 SEM images of RE-added dendritic micro-nano α-Fe fractals: a) Fe-1La, b) Fe-4La, c) Fe-1Ce and d) Fe-4Ce.

The transmission electron microscope (TEM) and high-resolution TEM (HRTEM) images in Figure 2 clearly show the refined structure and morphologies of Fe-4La and Fe-4Ce. Both Fe-4La and Fe-4Ce are about 6 μm long and about 1.5 μm wide. Their branches and trunks become bent and asymmetrical compared with that of unadded or less-added dendritic α-Fe samples. In addition, HRTEM micrographs show that there are a lot of nano-sized particles on the surface of the branches and tips (Figure 2b, e, f) which could provide plentiful grain boundaries (the boundaries among nanosized particles). We propose that these particles are the result of suppression effect of RE ions [33]. Also, these generated nano-sized particles could suppress the growth of the dendritic α-Fe and promote the formation of the unique multi-nanoparticles structure, which could further decrease their size and provide plentiful grains boundaries (Figure S3). However, because the main segments of trunks grow along [110] directions, as shown in Figure 2c, the samples still keep the similar dendritic shape. Selected area electron diffraction (SAED) patterns (Figure S4) indicate that the crystals are polycrystalline structure for those dendritic samples as shown in Figure 2a and 2d.

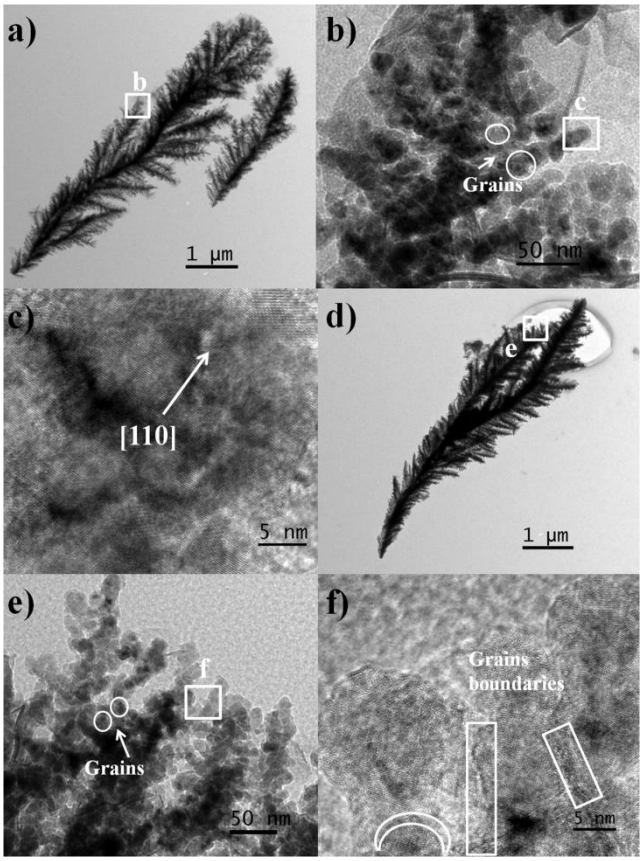

Fig. 2 TEM and HRTEM images of (a, b and c) Fe-4La and (d, e and f) Fe-4Ce dendritic micro-nano structure α-Fe fractal: (a, d) Low-magnification TEM images; (b, e) HRTEM images taken from the branches labeled as b) and e) in a) and d) , respectively; (c, f) HRTEM images taken from the areas labeled as (c and f) in b) and e), respectively.

XRD patterns (Figure 3a) indicates all these samples are indexed to body-centered cubic phase of α-Fe. With the increasing of adding amounts, the diffraction peaks become broad and their relative intensities decrease. It is well known that the peak broadening could be caused by a reduction in crystallite size and/or an increase in lattice strain.[34] Therefore, this change may be another evidence for the formation of nano-sized particles. According to the Brunauer–Emmett–Teller (BET) theory, the BET surface areas of La-added and Ce-added samples were calculated from N_2 adsorption-desorption isotherms (Figure S5). It is rising from about 10 m^2 g^{-1} of unadded samples to 40.5 m^2 g^{-1} of Fe-4La and 45.2 m^2 g^{-1} of Fe-4Ce (Figure 3d). The increase of the surface area results from the smaller size and the nano-sized particles after adding more RE ions agents in the electrolyte.

Based on the adsorption suppression effect of RE elements, we propose a possible formation mechanism of nano-sized particles. During the reaction process, the Fe^{2+} ions are reduced and deposited on the electrode surface as illustrated in our previous work report. But in here, the RE^{3+} ions are also enriched on cathode surface under the electric field force and further adsorbed on the surface of cathode and generated dendritic α-Fe due to their strong adsorption effect stemming from RE ions special 4*f* atomic orbits[35, 36], which further suppress the dendritic structure growth and distort the growth direction. The cathodic polarization curves (Figure S6) indicate that at the high polarization current density, RE-added samples show higher over-potentials than unadded samples, which also confirm that RE ions play a role in suppressing the deposition of Fe^{2+}. Due to the low standard reduction potential and the very low ions concentration of RE^{3+}, they cannot be reduced from the electrolyte and enter the crystal lattice of iron. The amount of RE elements in the sample is lower than 0.78 *wt*. % (Table S1), which is from the adsorbed RE elements on the samples' surface. This novel crystal structure is quite important to the chemical and physical properties of dendritic micro-nano materials.

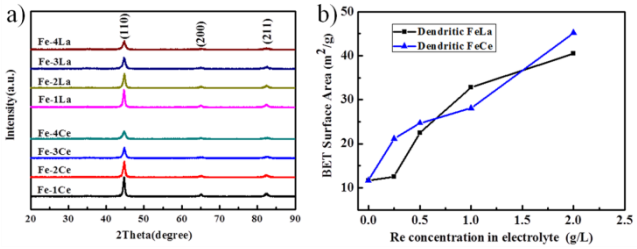

Fig. 3 a) XRD patterns of La-added and Ce-added dendritic micro-nano structure α-Fe; b) BET surface area of dendritic micro-nano structure α-Fe synthesized with different RE ions concentration.

In order to elucidate the magnetic properties of multi-grains boundaries dendritic micro-nano structure α-Fe, their static magnetic properties were measured by Vibrating Sample Magnetometer at room temperature, and their Magnetic hysteresis (*M*-*H*) loops are given in Figure S7. The results (in Figure 4) indicate that the La-added and Ce-added dendritic α-Fe display the similar variation tendency for saturation magnetization (*M*s) and coercivity (*H*c) values. With the increase of RE ions concentration in electrolyte, the *M*s value decreases from 215.46 $emug^{-1}$ of Fe-1La to 109.53 $emug^{-1}$ of Fe-4La; for the Ce-added samples, the *M*s value also reaches the minimum of 117.77 $emug^{-1}$ for Fe-4Ce. This decrease possibly results from the increased volume of the grain boundaries of the RE-added samples.[37, 38]

However, the *H*c value has the inverse tendency compared with *M*s. It increases from about 330 Oe for Fe-1La and Fe-1Ce to the maximum of 571.8 Oe (Fe-4La) and 624.56 Oe (Fe-4Ce) respectively. The larger *H*c value is attributed to the electron structure, shape anisotropy and hierarchical structure of the RE-added dendritic α-Fe synthesized under nonequilibrium state.[39-41] Magnetic material with a large coercive field (*H*c) is expected to show a high-frequency resonance.[42] So we predict that the sample containing more adding amounts would have stronger absorption on high-frequency region.

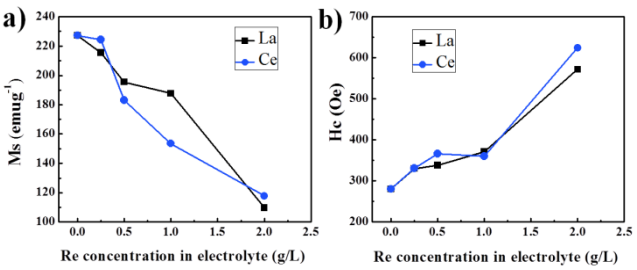

Fig. 4 a) Saturation magnetization (*M*s) and b) coercivity (*H*c) plots of the La-added and Ce-added dendritic micro-nano structure α-Fe synthesized in electrolyte with different RE concentrations.

Figure 5 shows the complex relative permittivity ($\varepsilon_r=\varepsilon'-j\varepsilon''$, ε'

and ε'' are the real and imaginary part of complex permittivity) and permeability ($\mu_r=\mu'-j\mu''$, μ' and μ'' are the real and imaginary part of complex permeability) of La-added and Ce-added dendritic micro-nano structure α-Fe. From Figure 5 we can know that complex relative permittivity and permeability of all the samples have the similar shape due to their pristine electromagnetic properties. However, both La and Ce adding could obviously alter the complex relative permittivity and permeability simultaneously on value under some specific frequency. For La-added and Ce-added samples, the ε' and ε'' values of dendritic micro-nano structure α-Fe are larger than that of unadded samples [29] in the whole frequency range. Meanwhile, the μ' values keep the similar tendency to that of pure sample in the almost whole frequency rang. The μ'' values decrease clearly with the increase of RE ions concentration, especially between 2 to 9 GHz. The plentiful grains boundaries which act as the electric charge centers [43] in the samples could enhance the polarization and decrease the electrical conductivity. At the same time, the exchange energy and anisotropy energy also are changed by the plentiful grains boundaries.[44] These changes result in the variety of complex relative permittivity and permeability after adding RE elements.

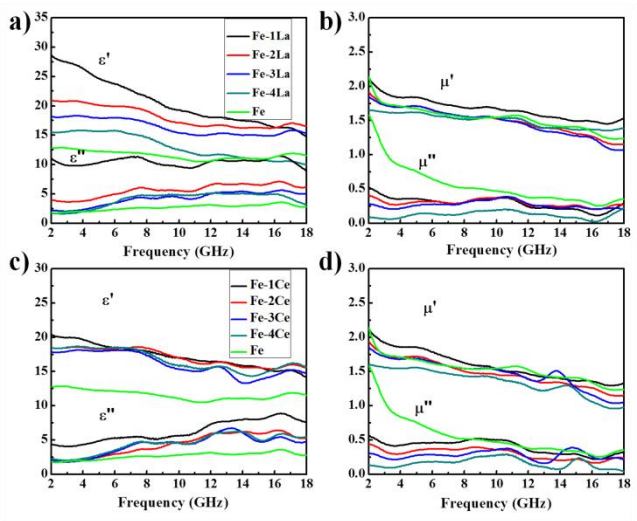

Fig. 5 Frequency dependence of real parts and imaginary parts of (a, c) complex relative permittivity and (b, d) complex relative permeability of La-added, Ce-added and unadded dendritic micro-nano structure α-Fe.

Specially, for La-added dendritic α-Fe samples (Figure 5a, b), with the increase of La^{3+} concentration, the response peak of ε'' at about 16.5 GHz weakens, and the response peak of μ'' at about 17.6 GHz strengthens. For Ce-added samples, they have a more significant influence on the complex relative permeability. Two response peaks of ε'' and ε' (shown in the Figure 5c) on 12-14 GHz and 16-18 GHz appear and strengthen with Ce^{3+} content increasing. Most importantly, an interesting response peak on μ' and μ'' spectrums (Figure 5d) appears between about 13 GHz and 17 GHz for both Fe-3Ce and Fe-4Ce. It indicates that the exchange resonance of Fe-3Ce and Fe-4Ce are enhanced dramatically. These changes attribute to the enhancement of the energy anisotropy of the sample [45], which affect their response frequency and resonance behaviours. In addition, we propose that all of these differences in complex relative permittivity and permeability between La-added and Ce-added samples may result from the different properties and orbits structure of La and Ce atomics adsorbed on the samples' surface.

To evaluate the electromagnetic absorption performance of multi-grains boundaries dendritic micro-nano structure α-Fe, the reflection loss (RL) values were calculated through Equation (1) and (2)[15, 46]:

$$RL(dB)= -20\log\frac{|Z_{in}-1|}{|Z_{in}+1|} \quad (1)$$

$$Z_{in}=\sqrt{\frac{\mu_r}{\varepsilon_r}}\tanh\left[j\cdot\frac{2\pi}{c}\sqrt{\mu_r\cdot\varepsilon_r}\cdot f\cdot d\right] \quad (2)$$

Where ε_r and μ_r are the complex relative permittivity and permeability, *f* is the applied frequency, *c* is the velocity of light, and *d* is the thickness of composites. The calculated results are shown in Figure 6 and 7, respectively.

In Figure 6, the minimum RL value of Fe-1La is -12.5 dB at 2 GHz with a 4.8 mm thickness. When the La^{3+} concentration in electrolyte is 1.00 g Ł$^{-1}$, the RL value decreases to the minimum (-62.1 dB) at about 3.5 GHz with the thickness of 3.3 mm. As the La^{3+} concentration continues increasing, the minimum RL value keeps around -60 dB, and the absorption peaks shift towards higher frequency (6-10 GHz) with a thinner thickness of about 2.0 mm. The widest absorption band (in which RL< -20 dB) jumps from 0 of Fe-1La to about 0.5 GHz of Fe-2La with the thickness of 2.5 mm, and then reaches the maximum of more than 2 GHz of Fe-4La with the thickness of 1.2 mm. In Figure 7, the minimum RL value drops from -34 dB at about 2.3 GHz to -66.5 dB at about 7.5 GHz when the Ce^{3+} concentration in electrolyte increases from 0.25 g Ł$^{-1}$ to 2.00 g Ł$^{-1}$. Meanwhile, the corresponding thickness decreases from about 5.0 mm to 2.0 mm. However, the width of absorption band is becoming narrower and narrower with Ce^{3+} content increasing, from 1 GHz of Fe-1Ce to about 0.5 GHz of other three Ce-added samples. In addition, another absorption peak apears in the range of 16-18 GHz when the RE ions concentration in electrolyte reaches 2.00 g Ł$^{-1}$, as shown in Figure 6d and 7d. In short, both of La-added and Ce-added samples' minimum RL values are superior to the unadded dendritic α-Fe samples (RL_{min}= -32.4dB, absorption band width=1.5 GHz, Thickness= 1.5 mm)[29]. The absorption band width of Fe-4La also obviously wider than that of unadded sample. Further more, The electromagnetic absorption performance of RE added dendritic α-Fe samples is superior to many other modified metal based absorbers (such as, Ag encapsulated Fe@SiO_2[47], Ni@TiO_2 and Ni@SiO_2[48]), of which RL_{min} is -40dB and maximum width of absorption band (in which RL< -10 dB) reaches 3.5 GHz.

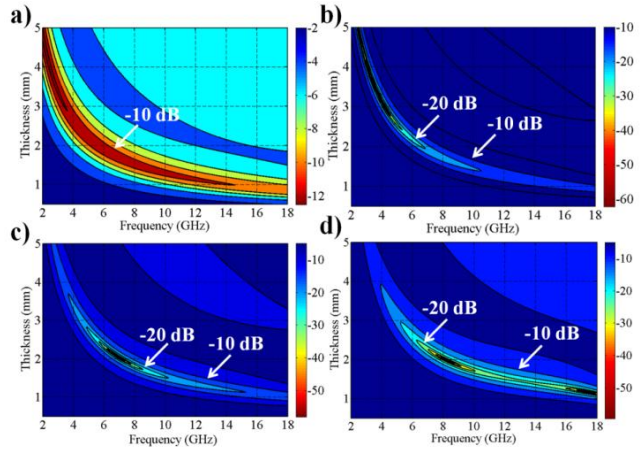

Fig. 6 EMA performance of a) Fe-1La, b) Fe-2La, c) Fe-3La, and d) Fe-4La samples which were mixed with paraffin under different thickness in the 2-18 GHz frequency range.

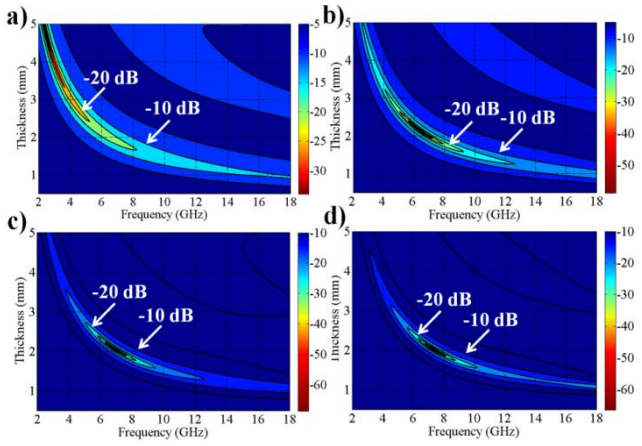

Fig. 7 EMA performance of a) Fe-1Ce, b) Fe-2Ce, c) Fe-3Ce, and d) Fe-4Ce samples which were mixed with paraffin with different thickness in the 2-18 GHz frequency range.

From the above results, we propose that the excellent EMA performance is attributed to the influence of RE ions by adjusting the refined dendritic structure and size. The adsorption suppression effect of RE ions in the electrolyte could lead to the generation of plentiful nanosized particles and decrease the size of the synthesized samples. The large BET surface area could increase the interfacial polarization between conductive absorber and insulating paraffin[49, 50]. More importantly, the abundant nanosized particles on the RE-added dendritic α-Fe would provide more grain boundaries which could also act as polarized centers and further enhance the polarization ratio.[19, 51, 52] Therefore, we propose that the abundant grains boundaries could enhance the dielectric loss of samples dramatically.

What's more, the formation of plentiful nanosized particles also affects the magnetic properties, and further affects the magnetic loss.[44] The plentiful nanosized grains on the hierarchical dendritic morphological α-Fe contribute to enhancing the shape anisotropy field (H_a) which is a key factor related to the resonance frequency.[53] According to the natural resonance equation: $2\pi f_r = \nu H_a$, where ν is the gyromagnetic ratio,[42] the added Re elements make the ferromagnetic response peaks shift to the high-frequency band[18]. We propose that the response peak located between 8 GHz and 12 GHz may be ascribed to nature resonance (Figure S8 b and d). Meanwhile, the response peaks between 13 GHz and 17 GHz in magnetic loss tangents curves of Fe-3Ce and Fe-4Ce are strengthened dramatically because of the enhance of exchange resonance[54].

Conclusions

In this work, the multi-grains boundaries hierarchical dendritic micro-nano structure α-Fe was successfully synthesized. RE adding obviously affects the dendritic structure and size due to its suppression effect on crystal growth. With the increase of RE ions contents, dendritic α-Fe become smaller and meanwhile plentiful nanosized particles generate on their surface, which lead to the distinct increase of BET surface area and the generation of the abundant grains boundaries. The abundant grain boundaries and large BET surface area are contributed to improving the polarization centers and increasing the interfacial polarization. Moreover, these nanosized particles could also increase the magnetic shape anisotropy, which change the resonance behavior and make the response frequency move towards high-frequency range. The results show that the minimum RL could reach -66.5 dB for Fe-4Ce, and the widest absorption band, in which RL< -20 dB, is 2 GHz for Fe-4La. Obviously, EMA performances are dramatically enhanced in absorption efficiency and absorption band width, compared with the unadded dendritic α-Fe and many of other electromagnetic absorbers.

This work offers a novel idea to enhance the electromagnetic absorption performance by changing their microstructure and morphology. Meanwhile, it provides a meaningful way to control the morphology and structure of the products by adding RE ions in the electrolyte. It will extend the application of the RE elements dramatically in the electromagnetic absorption area and crystal structure control area.

Acknowledgements

This work is supported by State Key Laboratory of Urban Water Resource and Environment (Harbin Institute of Technology) (No. 2013DX06)

Notes

State Key Laboratory of Urban Water Resource and Environment, School of Chemical Engineering and Technology, Harbin Institute of Technology, Harbin 150001, China
Tel:+86-451-86402805; Fax:+86-451-86418270
E-mail: jiangzhaohua@hit.edu.cn

† Electronic Supplementary Information (ESI) available: [More SEM, HRTEM and SAED images of RE-added dendritic micro-nano α-Fe, specific ICP-OES data, the N_2 adsorption-desorption isotherms, cathodic polarization curves and magnetic hysteresis (*M-H*) loops of all the RE added dendritic micro-nano α-Fe, and the calculated dielectric loss and magnetic loss are given]. See DOI: 10.1039/b000000x/

References

1. A. Ahlbom and M. Feychting, *British Medical Bulletin*, 2003, **68**, 157-165.
2. D. Formica and S. Silvestri, *BioMedical Engineering OnLine*, 2004, **3**, 11.
3. V. M. Petrov and V. V. Gagulin, *Inorg. Mater.*, 2001, **37**, 93-98.
4. D. D. L. Chung, *Carbon*, 2001, **39**, 279-285.
5. D. Zhang, F. Xu, J. Lin, Z. Yang and M. Zhang, *Carbon*, 2014, **80**,

103-111.
6. L. Yan, J. Wang, X. Han, Y. Ren, Q. Liu and F. Li, *Nanotechnology*, 2010, **21**, 095708.
7. C. Gong, X. Wang, X. Zhang, X. Zhao, H. Meng, Y. Jia, J. Zhang and Z. Zhang, *Mater. Lett.*, 2014, **121**, 81-84.
8. X. G. Liu, D. Y. Geng, H. Meng, P. J. Shang and Z. D. Zhang, *Appl. Phys. Lett.*, 2008, **92**, 173117.
9. C.-L. Zhu, M.-L. Zhang, Y.-J. Qiao, G. Xiao, F. Zhang and Y.-J. Chen, *J. Phys. Chem. C*, 2010, **114**, 16229-16235.
10. Y.-J. Chen, P. Gao, R.-X. Wang, C.-L. Zhu, L.-J. Wang, M.-S. Cao and H.-B. Jin, *J. Phys. Chem. C*, 2009, **113**, 10061-10064.
11. Q. Yuchang, Z. Wancheng, J. Shu, L. Fa and Z. Dongmei, *Physica B: Condensed Matter*, 2011, **406**, 777-780.
12. Y. J. Chen, P. Gao, C. L. Zhu, R. X. Wang, L. J. Wang, M. S. Cao and X. Y. Fang, *J. Appl. Phys.*, 2009, **106**, 054303.
13. X.-L. Shi, M.-S. Cao, J. Yuan, Q.-L. Zhao, Y.-Q. Kang, X.-Y. Fang and Y.-J. Chen, *Appl. Phys. Lett.*, 2008, **93**, 183118.
14. Y. Chen, Z. Lei, H. Wu, C. Zhu, P. Gao, Q. Ouyang, L.-H. Qi and W. Qin, *Mater. Res. Bull.*, 2013, **48**, 3362-3366.
15. Q. Liu, D. Zhang and T. Fan, *Appl. Phys. Lett.*, 2008, **93**, 013110.
16. R. C. Che, C. Y. Zhi, C. Y. Liang and X. G. Zhou, *Appl. Phys. Lett.*, 2006, **88**, 033105.
17. H. Yu, T. Wang, B. Wen, M. Lu, Z. Xu, C. Zhu, Y. Chen, X. Xue, C. Sun and M. Cao, *J. Mater. Chem.*, 2012, **22**, 21679-21685.
18. X. F. Zhang, X. L. Dong, H. Huang, B. Lv, J. P. Lei and C. J. Choi, *J. Phys. D: Appl. Phys.*, 2007, **40**, 5383.
19. Y. Ren, C. Zhu, S. Zhang, C. Li, Y. Chen, P. Gao, P. Yang and Q. Ouyang, *Nanoscale*, 2013, **5**, 12296-12303.
20. A. P. Singh, P. Garg, F. Alam, K. Singh, R. B. Mathur, R. P. Tandon, A. Chandra and S. K. Dhawan, *Carbon*, 2012, **50**, 3868-3875.
21. X.-J. Zhang, G.-S. Wang, W.-Q. Cao, Y.-Z. Wei, J.-F. Liang, L. Guo and M.-S. Cao, *ACS Appl. Mater. Interfaces*, 2014, **6**, 7471-7478.
22. X. Luo, G.-S. Wang, H.-Y. Guo, X.-J. Zhang, W.-Q. Cao, Y.-Z. Wei, L. Guo and M.-S. Cao, *ChemPlusChem*, 2014, **79**, 1089-1095.
23. Q. Wang, Z. Lei, Y. Chen, Q. Ouyang, P. Gao, L. Qi, C. Zhu and J. Zhang, *J. Mater. Chem. A*, 2013, **1**, 11795-11801.
24. J. K. Nelson and J. C. Fothergill, *Nanotechnology*, 2004, **15**, 586.
25. G.-S. Wang, S. He, X. Luo, B. Wen, M.-M. Lu, L. Guo and M.-S. Cao, *RSC Adv.*, 2013, **3**, 18009-18015.
26. J.-r. Liu, M. Itoh, M. Terada, T. Horikawa and K. Machida, *Appl. Phys. Lett.*, 2007, **91**, 093101.
27. S.-S. Kim, S.-T. Kim, Y.-C. Yoon and K.-S. Lee, *J. Appl. Phys.*, 2005, **97**, 10F905.
28. G. Sun, B. Dong, M. Cao, B. Wei and C. Hu, *Chem. Mater.*, 2011, **23**, 1587-1593.
29. Z. Yu, Z. Yao, N. Zhang, Z. Wang, C. Li, X. Han, X. Wu and Z. Jiang, *J. Mater. Chem. A*, 2013, **1**, 4571-4576.
30. J. Kong, S. Shi, L. Kong, X. Zhu and J. Ni, *Electrochim. Acta*, 2007, **53**, 2048-2054.
31. Y. Liu, H. Liu, J. Ma and J. Li, *Electrochim. Acta*, 2011, **56**, 1352-1360.
32. Z. Yu, N. Zhang, Z. Yao, X. Han and Z. Jiang, *J. Mater. Chem. A*, 2013, **1**, 12462-12470.
33. D. Wang, Y. Cheng, H. Jin, J. Zhang and J. Gao, *J. Rare Earth.*, 2013, **31**, 209-214.
34. O. M. Lemine, *Superlattices Microstruct.*, 2009, **45**, 576-582.
35. S. Guan and B. J. Nelson, *J. Magn. Magn. Mater.*, 2005, **292**, 49-58.
36. D. Wang, C. Wang, C. Dai and D. Sun, *Rare Met.*, 2006, **25**, 47-50.
37. M. Pękała, D. Oleszak, E. Jartych and J. K. Żurawicz, *Nanostruct. Mater.*, 1999, **11**, 789-796.
38. Y. Feng and T. Qiu, *J. Magn. Magn. Mater.*, 2012, **324**, 2528-2533.
39. D. A. Dimitrov and G. M. Wysin, *Phys. Rev. B*, 1995, **51**, 11947-11950.
40. S.-J. Park, S. Kim, S. Lee, Z. G. Khim, K. Char and T. Hyeon, *J. Am. Chem. Soc.*, 2000, **122**, 8581-8582.
41. P. Gambardella, S. Rusponi, M. Veronese, S. S. Dhesi, C. Grazioli, A. Dallmeyer, I. Cabria, R. Zeller, P. H. Dederichs, K. Kern, C. Carbone and H. Brune, *Science*, 2003, **300**, 1130-1133.
42. S.-i. Ohkoshi, S. Kuroki, S. Sakurai, K. Matsumoto, K. Sato and S. Sasaki, *Angew. Chem. Int. Ed.*, 2007, **46**, 8392-8395.
43. F. Greuter and G. Blatter, *Semicond. Sci. Technol.*, 1990, **5**, 111.
44. A. H. Taghvaei, H. Shokrollahi, M. Ghaffari and K. Janghorban, *J. Phys. Chem. Solids*, 2010, **71**, 7-11.
45. G. Rohrer, *J. Mater. Sci.*, 2011, **46**, 5881-5895.
46. P. A. Miles, W. B. Westphal and A. Von Hippel, *Rev. Mod. Phys.*, 1957, **29**, 279-307.
47. S. Senapati, S. K. Srivastava, S. B. Singh and A. R. Kulkarni, *Environ. Res.*, 2014, **135**, 95-104.
48. B. Zhao, G. Shao, B. Fan, W. Zhao and R. Zhang, *PCCP*, 2015, **17**, 2531-2539.
49. Y.-L. Ren, H.-Y. Wu, M.-M. Lu, Y.-J. Chen, C.-L. Zhu, P. Gao, M.-S. Cao, C.-Y. Li and Q.-Y. Ouyang, *ACS Appl. Mater. Interfaces*, 2012, **4**, 6436-6442.
50. J. Liu, J. Cheng, R. Che, J. Xu, M. Liu and Z. Liu, *ACS Appl. Mater. Interfaces*, 2013, **5**, 2503-2509.
51. T. Xia, C. Zhang, N. A. Oyler and X. Chen, *Adv. Mater.*, 2013, **25**, 6905-6910.
52. R. Che, L. Peng, X. Duan, Q. Chen and X. Liang, *Adv. Mater.*, 2004, **16**, 401-405.
53. B. W. Li, Y. Shen, Z. X. Yue and C. W. Nan, *J. Magn. Magn. Mater.*, 2007, **313**, 322-328.
54. T. Liu, Y. Pang, M. Zhu and S. Kobayashi, *Nanoscale*, 2014, **6**, 2447-2454.

TOC:

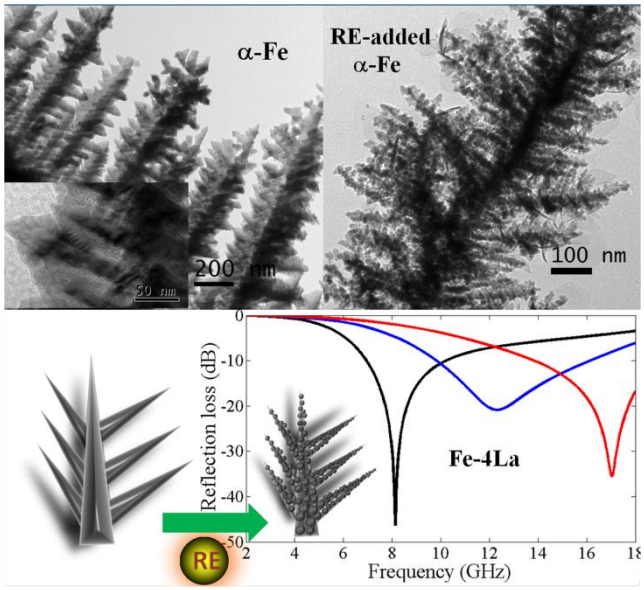

The Rare earth (RE) ions in the electrolyte could lead to the size decrease of the dendritic morphological α-Fe and the generation of multi-nanoparticles on their surface due to the adsorption suppression effect during growth process, which facilitates the significant increase of BET surface areas and grains boundaries. Not only do these nanosized particles improve the interfacial polarization and increase the polarization centers, but also affect their magnetic anisotropy field and resonance behaviours for electromagnetic wave, which dramatically enhance the electromagnetic absorption performance.